



1 **A new high-resolution pollen sequence at Lake Van, Turkey: Insights into penultimate interglacial-**
2 **glacial climate change on vegetation history**

3 Pickarski, Nadine¹ and Litt, Thomas¹

4 ¹ *University of Bonn, Steinmann Institute for Geology, Mineralogy, and Paleontology, Bonn, Germany*

5 *Correspondence to:* Nadine Pickarski (pickarski@uni-bonn.de)

6 **Abstract**

7 A new detailed pollen and oxygen isotope record of the penultimate interglacial-glacial cycle,
8 corresponding to the Marine Isotope Stage (MIS) 7-6 (c. 242.5-131.2 ka before present), has been
9 generated from the ‘Ahlat Ridge’ (AR) sediment core at Lake Van, Turkey. The presented record displays
10 the highest temporal resolution for this interval with a mean sampling interval of ~540 years.

11 Integration of all available proxies shows three intervals of effective moisture, evidenced by the
12 predominance of forested landscapes (oak-pine steppe forest), which can be correlated with MIS 7e, 7c,
13 and 7a. The warmest stage in terms of highest temperate tree percentages is MIS 7c, while the amplitude
14 of MIS 7e appears to be truncated by a shift to colder/drier climatic conditions. The detailed comparison
15 between the penultimate interglacial complex (MIS 7) to the last interglacial (Eemian, MIS 5e) and the
16 current interglacial (Holocene, MIS 1) provides a vivid illustration of possible differences of successive
17 climatic cycles. Intervening periods of open steppe landscape correlate with MIS 7d and 7a, favouring
18 local erosion and detrital sedimentation. The predominance of steppe elements during MIS 7d indicates
19 very cold/dry climatic conditions. In contrast, the occurrence of more temperate tree percentages
20 throughout MIS 7b points to relatively mild conditions, in agreement with atmospheric CO₂ concentration
21 and oxygen isotope records.

22 Despite the general dominance of dry/cold desert-steppe vegetation during the penultimate glacial (MIS
23 6), this period can be divided into two parts: an early stage (c. 193-157 ka BP) with pronounced
24 oscillations in tree percentages, and a later stage (c. 157-131 ka BP) with lower tree percentages and
25 subdued oscillations. The occurring vegetation pattern is analogous to the MIS 3 to MIS 2 division during
26 the last glacial in the same sediment sequence. Furthermore, we are able to identify the MIS 6e event (c.
27 179-159 ka BP) as described in marine pollen records, which indicates cooler but relatively wetter climate
28 conditions during the penultimate glacial.

29 In comparison with long European pollen records, speleothem isotope records from the Near East, and
30 global climate parameters (e.g., insolation, atmospheric CO₂ content), the new high-resolution Lake Van
31 record presents an improved insight into regional vegetation dynamics and climate variability in the
32 eastern Mediterranean region.



33 1. Introduction

34 The long continental pollen record of Lake Van (Turkey) contributes significantly to the picture of long-
35 term interglacial-glacial terrestrial vegetation history and climate conditions in the Near East (Litt et al.,
36 2014). Based on a lower time resolution, the 600,000 year old record already shows a general pattern of
37 alternating periods of forested and open landscapes that clearly responds to the Milankovitch-driven
38 global climatic changes (Berger, 1978; Martinson et al., 1987). In that study, the Lake Van pollen record
39 has demonstrated the potential ecological sensitivity for paleoclimate investigations that bridge the
40 southern European and Near East climate realms. Since then, high-resolution multi-proxy investigations of
41 the Lake Van sedimentary record allow the systematic documentation of different climatic phases
42 throughout the last interglacial-glacial cycle (Pickarski et al., 2015a, 2015b).

43 To date, little attention has been focused on characterizing terrestrial sedimentary archives beyond 130 ka
44 BP. In particular, the detailed vegetation response to climatic and environmental changes in the Near East
45 during the penultimate interglacial-glacial cycle (Marine Isotope Stage (MIS) 7 to 6) is not being
46 thoroughly investigated.

47 In this context, we present new high-resolution pollen and oxygen isotope data from the ‘Ahlat Ridge’
48 composite sequence over the penultimate interglacial-glacial cycle (between c. 242.5-131.2 ka BP). We
49 have added our recent results to the already available low-resolution palynological and isotope data from
50 Lake Van published by Litt et al. (2014) and Kwiecien et al. (2014). This enables us to provide new
51 detailed documentation of multiple vegetation and environmental changes in the Near East by a
52 centennial-to-millennial-scale temporal resolution of ~180 to 780 years. Our record is placed in its
53 regional context by the comparison with several archives from the Mediterranean region, e.g., Lake Ohrid
54 (between Former Yugoslavian Republic of Macedonia and Albania; Sadori et al., 2016), Ioannina basin
55 (NW Greece; Frogley et al., 1999; Roucoux et al., 2011, 2008; Tzedakis et al., 2003a), Tenaghi Philippon
56 (NE Greece; Tzedakis et al., 2006, 2003b), and Yammouneh basin (Lebanon; Gasse et al., 2015, 2011).

57 In this presented study, we want to address the following questions:

- 58 (I) What kind of regional vegetation occurs during the penultimate interglacial complex (MIS 7)?
59 Is the regional vegetation pattern of the MIS 7e comparable to the last interglacial (Eemian,
60 MIS 5e) and current warm stage (Holocene, MIS 1)?
- 61 (II) What processes characterize the climatic and environmental responses during MIS 6? Is this
62 vegetation history similar to the millennial-scale variability recorded during the last glacial
63 (MIS 4-2) in the same sequence?
- 64 (III) Does the Lake Van vegetation history correlate with other existing long pollen records from
65 southern Europe? What are the influencing factors of environmental change in the Near East?



66 Site description

67 Lake Van is situated on the eastern Anatolia high plateau at 1,648 m asl (meter above sea level; Fig. 1) in
68 Turkey. The deep terminal alkaline lake (~3,574 km², max. depth >450 m) occupies the eastern
69 continuation of the Muş basin developed in the collision zone between the Arabian and Eurasian plates at
70 ~13 Ma (Reilinger et al., 2006). Regional volcanism of Nemrut and Süphan volcanoes (at 2,948 m asl and
71 4,058 m asl, respectively, Fig. 1b), subaquatic hydrothermal exhalations and tectonic activities are still
72 active today, evident by the M 7.2 Van earthquake occurred on October 23, 2011 (Altiner et al., 2013).

73 The present-day climate at Lake Van is continental (warm dry summer and cool wet winter), with a mean
74 annual temperature of >9°C and mean annual precipitation between 400 and 1000 mm yr⁻¹ (Climate-
75 data.org, 1982-2012; Table 1). In general, eastern Anatolia receives most of its moisture in winter from
76 the eastern Mediterranean Sea. ‘Cyprus cyclones’ generated in the Mediterranean Sea or penetrating from
77 the North Atlantic are steered by the mid-latitudes westerlies and reinforced eastward along the northern
78 Mediterranean coast (Giorgi and Lionello, 2008). At Lake Van, rainfall decreases sharply from south-west
79 (c. 816 mm a⁻¹ in Tatvan) to north-east (c. 385 mm a⁻¹ in Van; Table 1) due to orographic effects of
80 NWW-SEE running Bitlis Massif parallel to the southern shore of the lake (Fig. 1).

81 Due to the diverse topography at Lake Van, local variations in moisture availability and temperature are
82 quite pronounced, reflected in the modern vegetation distribution. At present, the vegetation cover at Lake
83 Van has been altered by agricultural and pastoral activities. However, the southern mountain slopes are
84 characterized by an open deciduous oak shrubs and parklike steppe-forest containing *Quercus brantii*, *Q.*
85 *ithaburensis*, *Q. libani*, *Q. robur*, *Q. petraea*, *Juniperus excelsa*, and *Pistacia atlantica*, which is also
86 known as the Kurdo-Zagrosian vegetation. In contrast, the northern catchment area at Lake Van is
87 dominated by a dwarf-shrub steppes of *Artemisietea fragrantis anatolica*, also referred to as the Irano-
88 Turanian steppe and desert vegetation (Zohary, 1973).

89 2. Material and methods

90 2.1 Ahlat Ridge composite record

91 The sediment archive ‘AR’ (Ahlat Ridge; 38.667°N, 42.669°E at c. 357 m water depth, Fig. 1) was
92 collected during the drilling ICDP campaign (International Continental Scientific Drilling Program)
93 ‘PALEOVAN’ in summer 2010 (Litt and Anselmetti, 2014; Litt et al., 2012). The c. 219 mcbf (meter
94 composite below lake floor) record contains a well-preserved partly laminated or banded sediment
95 sequence, intercalated by several volcanic and event layers (e.g., turbidites; Stockhecke et al., 2014b). For
96 further detailed description of the Lake Van lithology, we refer to Stockhecke et al. (2014b).

97 In this paper, we focus on a 54.7 m long sediment section from 112.74 to 58.09 mcbf representing the
98 time span from c. 241.39 - 131.21 ka BP. In this section, we combine new pollen and isotope data with



99 those already obtained from the low-resolution pollen record (Litt et al., 2014) and oxygen isotopes data
100 derived from bulk sediments ($\delta^{18}\text{O}_{\text{bulk}}$; Kwiecien et al., 2014).

101 2.2 Chronology

102 The analytical approaches applied for the Lake Van chronology have previously been published in detail
103 in Stockhecke et al. (2014a). Main results of the construction of the age-depth model are briefly
104 summarized here.

105 For the investigated period, the age model is based on independent proxy records, e.g., on high-resolution
106 X-ray fluorescence (XRF) measurements (Kwiecien et al., 2014), total organic carbon (TOC; Stockhecke
107 et al., 2014b), and pollen data (Litt et al., 2014). The chronology was improved by adding two
108 paleomagnetic time markers (relative paleointensity minima, RPI), analyzed by Vigliotti et al. (2014), at
109 ~213-210 ka BP (Pringle Fall event; Thouveny et al., 2004) and at ~240-238 ka BP (Mamaku event;
110 Thouveny et al., 2004). In addition, three reliable $^{40}\text{Ar}/^{39}\text{Ar}$ ages of single crystal dated tephra layer at c.
111 161.9 ± 3.3 ka BP (V-114 at 71.48 mcbf), c. 178.0 ± 4.4 ka BP (V-137 at 82.29 mcbf), and c. 182 ka BP
112 (V-144 at 87.62 mcbf; Stockhecke et al., 2014b) are used to refine the age-depth model. For the final
113 chronology of this presented period, the composite record was correlated by using eight 'age control
114 points' derived from visual synchronization with the speleothem-based synthetic Greenland record (GL_{T}
115 $_{\text{syn}}$ from 116 to 400 ka BP; Barker et al., 2011).

116 2.3 Palynological analysis

117 For the new high-resolution pollen analysis, 193 sub-samples were taken at 20 cm intervals. The temporal
118 resolution between each pollen sample, derived from the present age-depth model, ranges from 180 to 780
119 years (mean temporal resolution c. 540 years).

120 Sub-samples of 4 cm³ were prepared using the standard palynological procedures by Faegri and Iversen
121 (1989), improved at the University of Bonn. This preparation includes treatment with KOH (10 %, hot),
122 HCL (10 %, cold), HF (39 %, cold), acetolysis mixture (hot), and ultrasonic sieving to concentrate the
123 palynomorphs. In order to calculate the pollen and micro-charcoal (>20 μm) concentrations (grains cm⁻³
124 and particles cm⁻³, respectively), tablets of *Lycopodium clavatum* spore (Batch no. 483 216, Batch no.
125 177745) were added to each sample (Stockmarr, 1971). In all spectra, the average of ~540 pollen grains
126 was counted in each sample using a Zeiss Axio Lab.A1 light microscope. Terrestrial pollen taxa were
127 identified to the lowest possible taxonomic, using the recent pollen reference collections of the Steinmann-
128 Institute, Department of Paleobotany and Beug (2004), Moore et al. (1991), Punt (1976), Reille (1999,
129 1998, 1995). Furthermore, we followed the taxonomic nomenclature according to Berglund and Ralska-
130 Jasiewiczowa (1986).



131 Pollen results are given as a percentages and concentration diagram of selected taxa (Fig. 2). This includes
132 the total arboreal pollen (AP; trees & shrubs) and non-arboreal pollen (NAP; herbs) ratio (100 %
133 terrestrial pollen sum). In order to evaluate sea-surface conditions, dinoflagellate cysts and green algae
134 (e.g., *Pseudopediastrum boryanum*, *P. kawraiskyi*, *Pediastrum simplex*, *Monactinus simplex*) were
135 counted on the residues from preparation for palynological analyses. Percent calculation, cluster analysis
136 (CONISS, sum of square roots) to define pollen assemblage zones (PAZ), and construction of the pollen
137 diagram was carried out by using TILIA software (version 1.7.16; ©1991–2011 Eric C. Grimm).

138 2.4 Oxygen isotope analysis

139 Stable oxygen isotope measurements ($\delta^{18}\text{O}_{\text{bulk}}$) were made on bulk sediments samples with an authigenic
140 carbonate content of ~30 % (CaCO_3). Similar to the pollen analysis, 193 sub-samples were taken for the
141 new high-resolution isotope record at 20 cm interval within the penultimate interglacial-glacial cycle.
142 Before measurements, the samples were dried at c. 40°C for 2 days and homogenized by a mortar. The
143 isotope analyses were carried out at the Leibnitz-Laboratory, University of Kiel, using a Finnigan
144 GasBenchII with carbonate option coupled to a DELTAplusXL IRMS.
145 All isotope values are reported in per mil (‰), relative to the Vienna Pee Dee Belemnite (VPDB)
146 standard. The standard deviation of the analyses of replicate samples is 0.02 ‰ for $\delta^{18}\text{O}_{\text{bulk}}$.

147 3. New data from the Lake Van sequence

148 3.1. The high-resolution pollen record

149 The new palynological results from the penultimate interglacial-glacial cycle are presented in Fig. 2. In
150 addition, the main characteristics of each pollen zone and sub-zone and the interpretation of their inferred
151 dominant vegetation types are summarized in Table 2.

152 The low-resolution pollen sequence, shown in Litt et al. (2014), has already been divided into six pollen
153 assemblage superzones (PAS IIIc, IV, Va, Vb, Vc, VI). This study followed the criteria for the
154 classification of the pollen superzones as described in Tzedakis (1994 and references therein). Based on
155 the new detailed high-resolution pollen sequence compared to the record in Litt et al. (2014), the PAS IV,
156 Va and Vc can now be further subdivided into 13 pollen assemblage zones (PAZ).

157 The pollen diagram provides a broad view of alternation between regional deciduous forested and open
158 steppe landscapes. The three main forested phases (PAZ Va1, Va3, Vc2, and Vc3), where total arboreal
159 vegetation reaches percentages above 30 %, are predominantly represented by deciduous *Quercus* (max.
160 ~56 %), *Pinus* (max. ~26 %), *Betula* (max. ~8 %), and *Juniperus* (max. ~7 %). Mediterranean
161 sclerophylls, e.g., *Pistacia* cf. *atlantica*, are only present sporadically and at very low percentages. During
162 open non-forested periods, the most significant herbaceous taxa are the steppe elements Chenopodiaceae



163 (max. ~7 %), *Artemisia* (max. ~56 %), and further herbs, such as Poaceae (max. ~54 %), Tubuliflorae
 164 (max. ~13 %), and Liguliflorae (max. ~10 %).

165 Throughout the sequence, the total pollen concentration values vary between c. 1,700 and 52,000 grains
 166 cm^{-3} dominated mainly by steppic herbaceous pollen types. The highest tree concentration peaks occur
 167 during forested intervals in PAZ Va1, Va3, Vc2, and Vc3 (all above c. 5,000 grains cm^{-3}).

168 In total, six *Pediastrum* taxa were identified on Lake Van sediments. Fig. 2a presents only the most
 169 important *Pediastrum* species. The density of the thermophilic taxa *Pseudopediastrum boryanum* reaches
 170 maxima values (c. 5,500 coenobia cm^{-3}) during PAZ Vc2, whereas the cold-tolerant species
 171 *Pseudopediastrum kawraiskyi* occur during the PAZ IV4-2 (max. values c. 2,000 coenobia cm^{-3}).

172 Furthermore, we calculated dinoflagellate concentration (*Spiniferites* species; cysts cm^{-3}) in order to get
 173 additional information about environmental conditions of the lake water (Dale, 2001; Shumilovskikh et
 174 al., 2012; Fig. 2a). In this study, the concentration of dinoflagellates is high (500-2,000 cysts cm^{-3}) during
 175 non-forested periods, especially within PAZ IV1, IV3, IV5, Va2, and PAS Vb.

176 The microscopic charcoal concentrations range between 300 and ~3,000 particles cm^{-3} during non-forested
 177 phases when terrestrial biomass were relatively low (PAZ IV1-5, Va2, Vb and Vc1; Fig. 2a). During
 178 forested phases, the charcoal content reaches maxima values of c. 8,000 particles cm^{-3} (e.g., in PAZ Va3,
 179 Vc4-2).

180 3.2. The oxygen isotopic composition of Lake Van sediments

181 The general pattern of Lake Van isotope composition of bulk sediments shows very high amplitude. The
 182 $\delta^{18}\text{O}_{\text{bulk}}$ ranges from c. 5.9 ‰ to -4.6 ‰. Positive values occur between 250 and 244 ka, 238-222 ka, at
 183 215 ka; 213-203 ka, 192-190 ka, 189-182 ka, and mainly between 171-157 ka and 141-134 ka BP.
 184 Negative isotope composition ($\delta^{18}\text{O}_{\text{bulk}}$ below 0‰) can be observed at ~241 ka; 221-216 ka; 202-194 ka;
 185 at ~181 ka, 178-171 ka, and between 156 and 155 ka BP.

186 Previous studies at Lake Van (e.g., Kwiecien et al., 2014; Lemcke and Sturm, 1997; Litt et al., 2012,
 187 2009; Wick et al., 2003) have shown that the stable isotope signature of lake carbonates reflects complex
 188 interaction between both several regional climatic variables and local site-specific factors. Such climate
 189 variables are the moisture source, in this case the eastern Mediterranean Sea surface water and the storm
 190 trajectories coming from the Mediterranean Sea, as well as temperature changes. Furthermore, the lake
 191 water itself is related to the seasonality of precipitation (both rain and snowfall; water inflow) and
 192 evaporation processes in the catchment area. However, the Lake Van authigenic carbonate $\delta^{18}\text{O}_{\text{bulk}}$ values
 193 are primarily controlled by water temperature and isotopic composition of the lake water ($T+\delta^{18}\text{O}_w$;
 194 Kwiecien et al., 2014; Leng and Marshall, 2004; Roberts et al., 2008).

195 The $\delta^{18}\text{O}_{\text{bulk}}$ composition of the lake water becomes progressively more enriched during
 196 interglacial/interstadial periods and lighter during glacial/stadial stages (Fig. 3b). Sharp negative peaks at



197 Termination III (T III at 241.4 ka BP) and at the transition from stadial to pronounced interstadial periods
198 documents not only enhanced precipitation during winter months but also the significant contribution of
199 depleted snow melt/glacier meltwater during the summer months (Kwiecien et al., 2014; Roberts et al.,
200 2008).

201 **4. Discussion**

202 **4.1 The penultimate interglacial complex (MIS 7)**

203 The penultimate interglacial at Lake Van resembles other interglacial complexes (e.g., the last
204 interglacial/interstadial complex, MIS 5; Pickarski et al., 2015a, 2015b) with three remarkable arboreal
205 pollen peaks. Here, the first sub-stage MIS 7e is generally considered as the full interglacial. This general
206 pattern of three warm phases (MIS 7e, 7c, and 7a) is separated by two intervening cold intervals (stadials;
207 MIS 7d and 7b) comparable with the marine classification by Martinson et al. (1987).

208 ***Forested periods***

209 The Lake Van pollen sequence shows three pronounced steppe-forested intervals within MIS 7 that
210 display high moisture availability and/or warmer temperature (Fig. 2a, 3e). Here, the steppe-forest periods
211 of MIS 7e (242.5-227.4 ka BP), MIS 7c (216.3-207.6 ka BP), and MIS 7a (203.1-193.4 ka BP) followed
212 the classical vegetation pattern of early to late temperate stage. The vegetation succession starts with the
213 colonization of open habitats by pioneer trees, such as *Betula*, followed by sclerophyllous *Pistacia* cf.
214 *atlantica* and a gradual expansion of deciduous *Quercus*. The abrupt occurrence of the frost-sensitive
215 *Pistacia* at the beginning of each forested interval indicates summer dryness due to higher temperature and
216 evaporation regime, and mild winter temperature. Moreover, the fire activity rose at Lake Van when
217 global temperature increased and the vegetation communities changed. It is clearly visible by high
218 charcoal concentration up to 5,000 particles cm⁻³ (Fig. 3d). In addition, the most depleted (negative)
219 $\delta^{18}\text{O}_{\text{bulk}}$ values occur at the base of each early temperate stage. This rapid change reflects intensified
220 freshwater supply into the lake by melting of Bitlis glaciers in summer months and/or enhanced
221 precipitation during winter months (Kwiecien et al., 2014; Roberts et al., 2008).

222 The climate optima of each forested interval are characterized by the maximum development of oak
223 steppe-forests, where summer-green *Quercus* rises consistently above 20 %. In case of MIS 7e, the
224 climate optimum occurs between c. 240 and 237 ka BP. Independent of environmental conditions around
225 the lake, the presence of thermophilic algae (i.e., *Pseudopediastrum boryanum*), which occurred mainly
226 during MIS 7e, displays warm and eutrophic conditions within the lake. In addition, the oxygen isotope
227 composition of the lake water confirms the obvious climate change within the region. The gradual shift
228 from depleted to enriched $\delta^{18}\text{O}_{\text{bulk}}$ values indicates a change towards warm climate conditions with high



229 evaporation rates and/or decreased moisture availability (Kwiecien et al., 2014; Roberts et al., 2008).
230 Here, positive $\delta^{18}\text{O}_{\text{bulk}}$ values at Lake Van are attributed to evaporative ^{18}O -enrichment of the lake water
231 during the dry season. Furthermore, Kwiecien et al. (2014) described the relation between soil erosion
232 processes and the vegetation cover in the catchment area. Our new high-resolution pollen record validates
233 this hypothesis with high authigenic carbonate concentration (low terrestrial input) along with the
234 increased terrestrial vegetation cover density during the climate optimum (Fig. 3c).

235 The ensuing ecological succession at Lake Van is documented by high percentages of dry-tolerant and/or
236 cold-adapted coniferous species (e.g., *Pinus* and *Juniperus*) that suggests a cooling trend with summer-dry
237 environment during the late stage (Fig. 2a, 3e). However, we are aware of the fact that pine pollen was
238 mainly transported over several kilometers via wind into the basin. Nevertheless, the presented regional
239 vegetation composition in the pollen spectra clearly illustrates a cooling/drying trend that appears during
240 the time of minimum ice volume. In other words, before the substantial ice accumulation is evident in the
241 marine MD01-2447 record (Desprat et al., 2006). In light of these insights, the MIS 7e vegetation
242 succession shows a shift from temperate species to the predominance of conifer taxa. Similar features are
243 recorded in the last interglacial stage (MIS 5e; 131.2-111.5 ka BP; Fig. 4), where the shift indicates higher
244 continentality, in particular to high seasonal contrasts on land along with low moisture availability (Litt et
245 al., 2014; Pickarski et al., 2015a).

246 Such pattern of forest succession, mentioned above, is not as clearly developed in each forested intervals.
247 For example, MIS 7c does not show a clear *Pistacia* cf. *atlantica* phase or MIS 7a a distinct *Pinus* phase.
248 Furthermore, the different amplitudes of the deciduous tree development, e.g., weak oak steppe-forest re-
249 expansion during MIS 7a and 7e, mirrored significant variability in regional effective moisture content
250 and/or temperature. These differences stem from the variety of factors, e.g., changes in orbital parameters
251 reflected in insolation forcing. In the case of MIS 7a, the ice volume was larger than during MIS 7c
252 (Desprat et al., 2006). Nevertheless, a possible explanation for high deciduous *Quercus* percentages in
253 MIS 7a is the persistence of relatively large tree populations through the preceding stadial MIS 7b.

254 All three forested stages of the MIS 7 are clearly recorded in other long terrestrial pollen sequences from
255 Lebanon and southern Europe: (I) the Yammouneh record (Gasse et al., 2015), (II) the Tenaghi Philippon
256 sequence (Tzedakis et al., 2003b), (III) Ioannina basin (Roucoux et al., 2008), and (IV) the Lake Ohrid
257 sequence (Sadori et al., 2016). Fig. 5 shows that the Lake Van pollen record generally agrees with the
258 vegetation development of the Mediterranean region. However, we have to take into consideration that
259 most southern European sequences, e.g., the Ioannina basin, are situated near to refugial areas, in which
260 temperate trees persisted during cold stages (Bennett et al., 1991; Milner et al., 2013; Roucoux et al.,
261 2008; Tzedakis et al., 2002). For example, the Mediterranean sequences show the most floristically
262 diverse and complete forest succession during the MIS 7c (Follieri et al., 1988; Roucoux et al., 2008;
263 Sadori et al., 2016; Tzedakis et al., 2003b). In contrast, the Lake Van interstadial contains only the highest



264 amplitude of deciduous *Quercus* (peaked at 212.6 ka BP) of the entire sequence. In fact, deciduous
265 *Quercus* percentages reach the level of the last interglacial (MIS 5e) and the Holocene forested intervals,
266 representing the most humid and temperate period at Lake Van (Fig. 4; Litt et al., 2014). Preliminary
267 comparison with eastern Mediterranean pollen records suggest that the extent and the diversity of
268 vegetation development is clearly controlled by insolation forcing and associated climate regimes (high
269 summer temperature, high winter precipitation). Therefore, the difference in the deciduous *Quercus*
270 percentages might have resulted from higher Mid-June insolation during MIS 7c relative to MIS 7e
271 (similar to Holocene levels), despite lower atmospheric CO₂ content (c. 250 ppm, Fig. 5; Jouzel et al.,
272 2007; Lang and Wolff, 2011; Petit et al., 1999; Tzedakis, 2005). However, we cannot recognize a clear
273 interglacial-like vegetation succession within the MIS 7c with, e.g., the occurrence of the summer-
274 drought-resistant specie *Pistacia* cf. *atlantica*. In this case, there does not seem any reason to define the
275 MIS 7c as a full interglacial separate from MIS 7e.

276 *Non-forested periods*

277 The two stadial phases between the three forested intervals, MIS 7d (227.4-216.3 ka BP) and MIS 7b
278 (207.6-203.1 ka BP), are characterized by: (I) extensive steppe vegetation when tree growth was inhibited
279 either by dry/cold or low atmospheric CO₂ conditions, (II) high dinoflagellate concentration (probably a
280 species which tolerate high water salinity conditions; Fig. 2a), and (III) high regional mineral input
281 derived from the basin slopes (Fig. 3c).

282 Due to the strongest development of extensive semi-desert steppe plants (mainly Chenopodiaceae) and
283 massive reduction of temperate tree (AP c. 5 %, Fig. 2), the MIS 7d suggests considerable climate
284 deterioration and increased aridity. Furthermore, this stadial is marked by large ice volume and extremely
285 low global temperatures, documented by low CO₂ concentration (c. 200 ppm, Fig. 5) values that are nearly
286 as low as those of MIS 8 and 6 (McManus et al., 1999; Petit et al., 1999). Concerning the oxygen isotope
287 record, the MIS 7d documents a significant change towards lighter $\delta^{18}\text{O}_{\text{bulk}}$ values (up to -3.8 ‰; Fig. 3b)
288 that reflect reduced evaporation in the Lake Van catchment area. Such a cold and/or dry period within the
289 entire interglacial complex can also be recognized in all pollen sequences from Lebanon and southern
290 Europe. An exception is the Lake Ohrid record, which shows only a minor temperate tree decline (Sadori
291 et al., 2016).

292 In contrast, the MIS 7b stadial recognizes only a slight and short-term steppe-forest contraction. Although
293 the landscape at Lake Van was more open, moderate values of *Betula*, deciduous *Quercus* (up to 16 %) and
294 conifers (*Pinus*, *Juniperus*) formed steppe vegetation with still patchy pioneer and temperate trees.
295 The significantly larger temperate tree pollen percentages (AP c. 20 %) during the sub-stage 7b relative to
296 MIS 7d point to milder climate conditions. In addition, the continuous heavier oxygen isotope signature
297 confirms the assumption of milder conditions with 'higher' evaporation rates (Fig. 3b). Based on these



298 results, the Lake Van pollen archive mirrored the trends seen in various paleoclimatic archives (Fig. 5).
299 Indeed, a number of arboreal pollen sequences from the Mediterranean area and oxygen isotope records
300 suggest that the North Atlantic and southern European region (i.e., Ioannina basin; Roucoux et al., 2008)
301 did not experience severe climatic cooling during MIS 7b (Fig. 5; e.g., Bar-Matthews et al., 2003; Barker
302 et al., 2011; McManus et al., 1999; Petit et al., 1999). In addition, the global ice volume remains relatively
303 low during the MIS 7b in comparison with other stadial intervals with similarly low insolation values
304 (e.g., Petit et al., 1999; Shackleton et al., 2000). Vostok ice-core sequence also records a relatively ‘high’
305 CO₂ content (c. 230 ppm) supporting a slight decline of temperature compared with MIS 7d (McManus et
306 al., 1999; Petit et al., 1999).

307 *Comparison of past interglacials at Lake Van*

308 The comparison of the penultimate interglacial (MIS 7e) with the last interglacial (Eemian, MIS 5e;
309 Pickarski et al., 2015a) and the current interglacial (Holocene, MIS 1; Litt et al., 2009) provides the
310 opportunity to assess how different successive climate cycles can be (Fig. 4).

311 In general, all interglacial climate optima are characterized by the development of an oak steppe-forest,
312 which indicates high effective moisture. A dense vegetation cover reduces physical erosion of the
313 surrounding soils in the lake basin. Furthermore, the dominance of forested landscapes and productive
314 steppe environment leads to enhanced fire activity in the catchment. However, all interglacial intervals at
315 Lake Van recognize a delayed forest onset of c. 3,000 to 2,000 years, visible by the slow expansion of
316 deciduous *Quercus*, based on summer-dry conditions (Litt et al., 2009; Pickarski et al., 2015a). In
317 addition, the late temperate stage of both the penultimate and last interglacial is documented by
318 continental environments with warm evaporative summer conditions and a higher seasonality due to the
319 vegetation shift towards the predominance of *Pinus* (Pickarski et al., 2015a).

320 Despite the common vegetation succession from an early to late temperate stage, the three interglacial
321 maxima differ significantly. One important difference of the last two interglacial vegetation assemblages
322 is the absence of *Carpinus* during MIS 7e, compared to a distinct *Carpinus betulus* phase during MIS 5e
323 (Pickarski et al., 2015a). In general, *Carpinus betulus* usually requires high amounts of annual rainfall,
324 and relatively high annual summer temperature. However, deciduous *Quercus* is ‘less’ sensitive to
325 summer droughts compared to *Carpinus betulus* and a decrease in humidity would favor the development
326 of an oak steppe-forest. A change in temperature is difficult to assess because deciduous oaks at Lake Van
327 include many species with different ecological requirements. Therefore, general ‘cooler/wetter’ conditions
328 of the penultimate interglacial resulted in overall smaller abundance of temperate trees. Possible reasons
329 for this development could be reduced Mid-June insolation (lower than Holocene level) and moderately
330 lower interglacial CO₂ content (Lang and Wolff, 2011). Moreover, general lower temperature are
331 commonly associated with the persistence of larger volumes of continental ice (Shackleton et al., 2000).



332 Another important difference is the duration of each full interglacial period. According to Tzedakis
333 (2005), the beginning and duration of terrestrial temperate intervals in the eastern Mediterranean region is
334 closely linked to the amplitude of summer insolation maxima and less influenced by the timing of
335 deglaciation. Based on this assumption, the climate optimum of the penultimate interglacial (c. 9.6 ka) is
336 c. 4 ka shorter as the last interglacial interval at Lake Van (~13.5 ka, Pickarski et al., 2015a; Fig. 4).

337 **4.2 The penultimate glacial (MIS 6)**

338 Within the penultimate glacial stage (MIS 6; 193.4-131.2 ka BP), the general lower summer insolation
339 (Berger, 1978; Berger et al., 2007), increased global ice sheet extent (McManus et al., 1999), and
340 decreasing atmospheric CO₂ content (below 230 ppm; Petit et al., 1999; Fig. 5) are responsible for the
341 enhanced aridity and cooling in eastern Anatolia. Such observed climate deterioration is evident by the
342 dominance of semi-desert plants (e.g., *Artemisia*, *Chenopodiaceae*) and by the rapid decline in temperate
343 trees (AP <20 %) during this time. High erosional activity (low Ca/K ratio) and decreasing paleofire
344 activity ($\emptyset \sim 1,400$ particles cm⁻³) result from low vegetation cover density with low pollen productivity
345 (Fig. 2, 3). As an additional local factor, the strong deficits in available plant water were possibly stored as
346 ice/glaciers in the Bitlis mountains during the coldest phases.

347 During 193 and 157 ka BP, high-frequency oscillations in tree percentages between ~1 and 18 % can be
348 observed in the pollen record. Furthermore, the early penultimate glacial stage documents similar high-
349 amplitude variations in $\delta^{18}\text{O}_{\text{bulk}}$ values (c. -4 to 6 ‰), compared to the isotope signature of MIS 7 (Fig.
350 3b). However, such rapid change in temperate plant communities, e.g. at ~189.4 ka BP, resembles the
351 pattern of interstadial to stadial stages. It indicates unstable environmental conditions with rapid
352 alternation of slightly warmer/wetter interstadials and cooler/drier stadials at Lake Van. This situation is
353 also reflected in several Lake Van paleoenvironmental proxies. Here, the short-term expansion of trees
354 and shrubs (deciduous *Quercus*, *Betula*, *Ulmus*, *Pinus*, and *Juniperus*; PAZ IV6, Fig. 2a, 3e) combined
355 with rapid variations in the fire intensity (up to 6,000 particles cm⁻³, Fig. 3e) and decreasing terrestrial
356 input of soil material (Fig. 3c), point to short-term humid conditions and/or low evaporation within
357 interstadials. Even if mean precipitation was low, the local available moisture was sufficient to sustain
358 arboreal vegetation when low temperature minimized evaporation. Nevertheless, the landscape around the
359 lake was still open and less extensive due to still high percentages of dry-climate adapted herbs.

360 In contrast, the period after 157 ka BP shows a great abundance of steppe elements with dwarf shrubs,
361 grasses and other herbs (e.g., *Chenopodiaceae*, *Artemisia*, *Ephedra distachya*-type) along with lower
362 temperate tree percentages (AP c. 1-8 %). The remaining tree values consist mainly of deciduous *Quercus*,
363 *Pinus*, with some scattered patches of *Betula* and *Juniperus*. The combination of minor AP oscillation,
364 high percentages of steppe plants (Fig. 2b), and reduced fire activity reflect a strong aridification and cold
365 continental climate during the late penultimate glacial. In addition, a general low-amplitude variation of



366 $\delta^{18}\text{O}_{\text{bulk}}$ values (c. -2 to 2 ‰; Fig. 3b) and local erosion processes (Fig. 3c) refer to a rather stable period
367 with both widespread aridity (low winter and summer precipitation) and low winter temperature across
368 eastern Anatolia.

369 The Lake Van record generally agrees with high-frequency paleoenvironmental variations in the ice-core
370 archives and high-resolution terrestrial European pollen records (e.g. Ioannina basin, Lake Ohrid; Fig. 5)
371 in terms of a general aridity and cooling throughout the penultimate glacial. Our sequence also share some
372 features with stable isotope speleothem records from western Israel (Peqi'in and Soreq Cave; Ayalon et
373 al., 2002; Bar-Matthews et al., 2003) concerning high $\delta^{18}\text{O}$ values that refers to dry climate conditions.
374 Similar to the Lake Van $\delta^{18}\text{O}_{\text{bulk}}$ values, the Soreq and Peqi'in record also show distinct climate
375 variability, especially at the beginning of the MIS 6 (Fig. 5). In addition, several high-resolution terrestrial
376 records document a further period of abrupt warming events between 155-150 ka BP. In particular, the
377 Tenaghi Philippon profile illustrates a prominent increase of up to 60 % in arboreal pollen, which
378 coincides with increase rainfall at Yammoûneh (Gasse et al., 2015) and at Peqi'in Cave (Bar-Matthews et
379 al., 2003).

380 *Comparison of the last two glacial intervals at Lake Van*

381 Compared to interglacial stages, forest vegetation cover was generally reduced during the glacial. The
382 occurrence of high-frequency climate changes within the Lake Van sediments provides an opportunity to
383 compare the vegetation history of the last two glacial periods. Fig. 6 illustrates that the first part of the
384 penultimate glacial (c. 193-157 ka BP) resembles MIS 3, regarding pronounced millennial-scale AP
385 oscillations and abruptness of the transition in the pollen record. The series of millennial-scale interstadial-
386 stadal intervals can be recognized in both glacial periods. This variability is mainly influenced by the
387 impact of North Atlantic current oscillations and the extension of atmospheric pattern, in particular,
388 northward shift of the polar front in eastern Anatolia (e.g., Cacho et al., 2000, 1999; Chapman and
389 Shackleton, 1999; McManus et al., 1999; Rasmussen et al., 2014; Wolff et al., 2010).

390 The longest and most distinct environmental variability occurs during MIS 6e (c. 179-159 ka BP), which
391 can be further divided into six interstadials based on rapid changes in the marine core MD01-2444 off
392 Portugal (Margari et al., 2010; Roucoux et al., 2011; Fig. 6). MIS 6e reveals a clear evidence of abrupt
393 climate variability due to rapid alternation in the vegetation cover similar to the largest Dansgaard-
394 Oeschger (DO) events 17 to 12 during MIS 3 (c. 60-44 ka BP; Pickarski et al., 2015b). Both intervals start
395 at the point of summer insolation maxima. Here, the Northern Hemisphere insolation values reach
396 interglacial level at the beginning of MIS 6e compared to the MIS 7e (Fig. 5). In contrast, the interstadial-
397 stadal pattern during the late MIS 6 oscillated at lower intensities, similar to rates of change in the
398 Dansgaard-Oeschger (DO) events during MIS 4 and 2, reflecting a general global climatic cooling.



399 Within the MIS 6e, the subdued temperate tree pollen oscillations consist mainly of deciduous *Quercus*
400 and *Pinus*, range between ~1 % and ~15 %. In contrast, the identical AP composition oscillates between
401 ~1 % and ~10 % during the orbitally equivalent MIS 3 (c. 61-28 ka BP). The different amplitude in
402 arboreal pollen percentages in both glacial stages and a general dense temperate grass steppe during the
403 MIS 6e is supported by more abundant summer moisture (Fig. 6). The general depleted isotope signature
404 may result from summer meltwater discharge from local glaciers (e.g., Taurus mountains, Bitlis Massif) or
405 by increased precipitation over the entire Mediterranean basin (Kallel et al., 2000). However, the presence
406 of *Artemisia* and *Poaceae* makes it difficult to disentangle the effects of warming from changes in
407 moisture availability in both glacials. Nevertheless, the occurrence of cold-tolerant taxa such as *Pinus*,
408 *Ephedra distachya*-type, and the algae *Pseudopediastrum kawraiskyi* points to a general picture of cold
409 but ‘wet’ climate conditions during MIS 6e than experienced during MIS 3.

410 Evidence for relatively humid but cold climate conditions during MIS 6e agrees with several other
411 paleoclimate studies from the Mediterranean area. For example, the occurrence of open forest vegetation
412 associated with wetter climate is indicated at, e.g., Tenaghi Philippon (Tzedakis et al., 2006, 2003b) and
413 Ioannina (Roucoux et al., 2011). In addition, the stalagmites record from the Soreq Cave (Israel) shows an
414 increase in precipitation (negative shift in the $\delta^{18}\text{O}$ values) in the eastern Mediterranean at ~177 and 166-
415 157 ka BP (Fig. 5; Ayalon et al., 2002; Bar-Matthews et al., 2003). Furthermore, a pluvial phase is also
416 inferred from a prominent speleothem $\delta^{18}\text{O}$ excursion in the Argentarola Cave (Italy) between 180 and
417 170 ka BP based on U/Th dating (Bard et al., 2002). This phase coincides with high runoff due to the
418 deposition of the ‘cold’ sapropel layer (S6, c. ~176 ka BP) in the western and eastern Mediterranean basin
419 (Ayalon et al., 2002; Bard et al., 2002). Finally, the progressive decline in effective moisture is a result of
420 the combined effect of temperature, precipitation and insolation changes in the Lake Van region.

421 5. Conclusions

422 The new high-resolution Lake Van pollen record provides a unique sequence of the penultimate
423 interglacial-glacial cycle that fills the gap in data coverage between the northern Levant and southern
424 Europe.

425 All climate-related variables at Lake Van varied at interglacial/interstadial-glacial/stadial scale. During the
426 MIS 7 complex, high local and regional effective moisture is evidenced by a dense temperate oak steppe-
427 forest, high charcoal accumulation, and reduced physical erosion during the climate optima. Each warm
428 stage is characterized by a succession of vegetation types: (I) pioneer and sclerophyllous taxa, (II)
429 temperate tree expansion dominated by deciduous *Quercus*, (III) *Pinus*-dominated landscapes, and (IV)
430 steppe vegetation. The comparison of past interglacials at Lake Van suggests wet and colder conditions
431 during the penultimate interglacial, strong thermal and hydrological seasonal contrasts during the last



432 interglacial, and a higher humidity during the Holocene climate optimum (at 6 ka cal. BP; Litt et al.,
433 2009).

434 During the penultimate glacial, a strong aridification and cold climate conditions are inferred from open
435 steppe vegetation that favors physical erosion and local terrigenous inputs. In particular, our record reveals
436 a pattern of subdued but ‘higher’ temperate oscillations between 193-157 ka BP, followed by a period of
437 lower tree variations and expansion of desert-steppe from 157-131 ka BP. A comparison between the last
438 two glacials highlights differences in vegetation responses in eastern Anatolia. The first part of MIS 6
439 including the MIS 6e event may point to cooler but relatively wetter conditions than experienced during
440 the MIS 3.

441 Finally, the eastern Mediterranean Lake Van pollen sequence is in line with data from long-term climate
442 records from southern Europe and the northern Levant, in terms of vegetation changes, orbitally-induced
443 fluctuations, global ice sheet waxing and waning, and atmospheric changes over the North Atlantic
444 system.

445 **Data availability:** The pollen data set is available online at... (www.pangaea.de).

446 **Acknowledgements**

447 Financial support was provided by the German Research Foundation (DFG; LI 582/20-1). We thank all
448 colleagues and scientific teams who have been involved in the Lake Van drilling, core opening and
449 sampling campaigns. We thank Dr. Nils Andersen and his working team at the Leibnitz-Laboratory for the
450 isotopic measurements. We thank Karen Schmeling for preparing excellent pollen samples, Christoph
451 Steinhoff and Helen Böttcher for their support in the lab. Special thanks go to Ola Kwiecien and Georg
452 Heumann for their critical reading of the manuscript and for the inspiring discussions. Patricia Pawlyk, as
453 a native speaker, is thanked for proof reading the English. We are grateful to Mira Bar-Matthews and
454 Avner Ayalon from the Geological Survey of Israel (Jerusalem) for the supply of the oxygen isotope data
455 of the Soreq and Peqi’in record.

456 **References**

- 457 Altiner, Y., Söhne, W., Güney, C., Perlt, J., Wang, R., Muzli, M., 2013. A geodetic study of the 23
458 October 2011 Van, Turkey earthquake. *Tectonophysics* 588, 118–134.
459 doi:10.1016/j.tecto.2012.12.005
- 460 Ayalon, A., Bar-Matthews, M., Kaufman, A., 2002. Climatic conditions during marine oxygen isotope
461 stage 6 in the eastern Mediterranean region from the isotopic composition of speleothems of
462 Soreq Cave, Israel. *Geology* 30, 303–306. doi:10.1130/0091-
463 7613(2002)030<0303:CCDMOI>2.0.CO;2
- 464 Bar-Matthews, M., Ayalon, A., Gilmour, M., Matthews, A., Hawkesworth, C.J., 2003. Sea–land oxygen
465 isotopic relationships from planktonic foraminifera and speleothems in the Eastern Mediterranean



- 466 region and their implication for paleorainfall during interglacial intervals. *Geochimica et*
 467 *Cosmochimica Acta* 67, 3181–3199. doi:10.1016/S0016-7037(02)01031-1
- 468 Bard, E., Delaygue, G., Rostek, F., Antonioli, F., Silenzi, S., Schrag, D.P., 2002. Hydrological conditions
 469 over the western Mediterranean basin during the deposition of the cold Sapropel 6 (ca. 175 kyr
 470 BP). *Earth and Planetary Science Letters* 202, 481–494. doi:10.1016/S0012-821X(02)00788-4
- 471 Barker, S., Knorr, G., Edwards, R.L., Parrenin, F., Putnam, A.E., Skinner, L.C., Wolff, E., Ziegler, M.,
 472 2011. 800,000 Years of Abrupt Climate Variability. *Science* 334, 347–351.
 473 doi:10.1126/science.1203580
- 474 Bennett, K.D., Tzedakis, P.C., Willis, K.J., 1991. Quaternary refugia of north European trees. *Journal of*
 475 *Biogeography* 103–115. doi:10.2307/2845248
- 476 Berger, A., 1978. Long-term variations of daily insolation and Quaternary climate changes. *Journal of*
 477 *Atmospheric Sciences* 35, 2362–2367. doi:10.1175/1520-
 478 0469(1978)035<2362:LTVODI>2.0.CO;2
- 479 Berger, A., Louté, M.F., Kaspar, F., Lorenz, S.J., 2007. Insolation During Interglacial, in: Sirocko, F.,
 480 Claussen, M., Sánchez Goñi, M.F., Litt, T. (Eds.), *The Climate of Past Interglacial*. Elsevier,
 481 Amsterdam, pp. 13–27.
- 482 Berglund, B.E., Ralska-Jasiewiczowa, M., 1986. Pollen analysis and pollen diagrams, in: Berglund, B.E.,
 483 Ralska-Jasiewiczowa, M. (Eds.), *Handbook of Holocene Palaeoecology and Palaeohydrology*.
 484 John Wiley and Sons, pp. 455–484.
- 485 Beug, H.-J., 2004. *Leitfaden der Pollenbestimmung für Mitteleuropa und angrenzende Gebiete*. Pfeil,
 486 München.
- 487 Cacho, I., Grimalt, J.O., Pelejero, C., Canals, M., Sierro, F.J., Flores, J.A., Shackleton, N., 1999.
 488 Dansgaard-Oeschger and Heinrich event imprints in Alboran Sea paleotemperatures.
 489 *Paleoceanography* 14, 698–705. doi:10.1029/1999PA900044
- 490 Cacho, I., Grimalt, J.O., Sierro, F.J., Shackleton, N.J. s, Canals, M., 2000. Evidence for enhanced
 491 Mediterranean thermohaline circulation during rapid climatic coolings. *Earth and Planetary*
 492 *Science Letters* 183, 417–429. doi:10.1016/S0012-821X(00)00296-X
- 493 Chapman, M.R., Shackleton, N.J., 1999. Global ice-volume fluctuations, North Atlantic ice-rafting events,
 494 and deep-ocean circulation changes between 130 and 70 ka. *Geology* 27, 795–798.
 495 doi:10.1130/0091-7613(1999)027<0795:GIVFNA>2.3.CO;2
- 496 Dale, B., 2001. The sedimentary record of dinoflagellate cysts: looking back into the future of
 497 phytoplankton blooms. *Scientia Marina* 65, 257–272. doi:10.3989/scimar.2001.65s2257
- 498 Desprat, S., Sánchez Goñi, M.F., Turon, J.-L., Duprat, J., Malaizé, B., Peyrouquet, J.-P., 2006. Climatic
 499 variability of Marine Isotope Stage 7: direct land–sea–ice correlation from a multiproxy analysis
 500 of a north-western Iberian margin deep-sea core. *Quaternary Science Reviews* 25, 1010–1026.
 501 doi:10.1016/j.quascirev.2006.01.001
- 502 Faegri, K., Iversen, J., 1989. *Textbook of Pollen Analysis*. The Blackburn Press.
- 503 Follieri, M., Magri, D., Sadori, L., 1988. 250,000-year pollen record from Valle di Castiglione Roma.
 504 *Pollen et Spores* 30, 329–356.
- 505 Frogley, M.R., Tzedakis, P.C., Heaton, T.H.E., 1999. Climate Variability in Northwest Greece During the
 506 Last Interglacial. *Science* 285, 1886–1889. doi:10.1126/science.285.5435.1886
- 507 Gasse, F., Vidal, L., Develle, A.-L., Van Campo, E., 2011. Hydrological variability in the Northern
 508 Levant: a 250 ka multiproxy record from the Yammouneh (Lebanon) sedimentary sequence.
 509 *Climate of the Past* 7, 1261–1284. doi:10.5194/cp-7-1261-2011
- 510 Gasse, F., Vidal, L., Van Campo, E., Demory, F., Develle, A.-L., Tachikawa, K., Elias, A., Bard, E.,
 511 Garcia, M., Sonzogni, C., Thouveny, N., 2015. Hydroclimatic changes in northern Levant over the
 512 past 400,000 years. *Quaternary Science Reviews* 111, 1–8. doi:10.1016/j.quascirev.2014.12.019
- 513 Giorgi, F., Lionello, P., 2008. Climate change projections for the Mediterranean region. *Global and*
 514 *Planetary Change* 63, 90–104. doi:10.1016/j.gloplacha.2007.09.005
- 515 Jouzel, J., Masson-Delmotte, V., Cattani, O., Dreyfus, G., Falourd, S., Hoffmann, G., Minster, B., Nouet,
 516 J., Barnola, J.M., Chappellaz, J., Fischer, H., Gallet, J.C., Johnsen, S., Leuenberger, M.,
 517 Loulergue, L., Luethi, D., Oerter, H., Parrenin, F., Raisbeck, G., Raynaud, D., Schilt, A.,



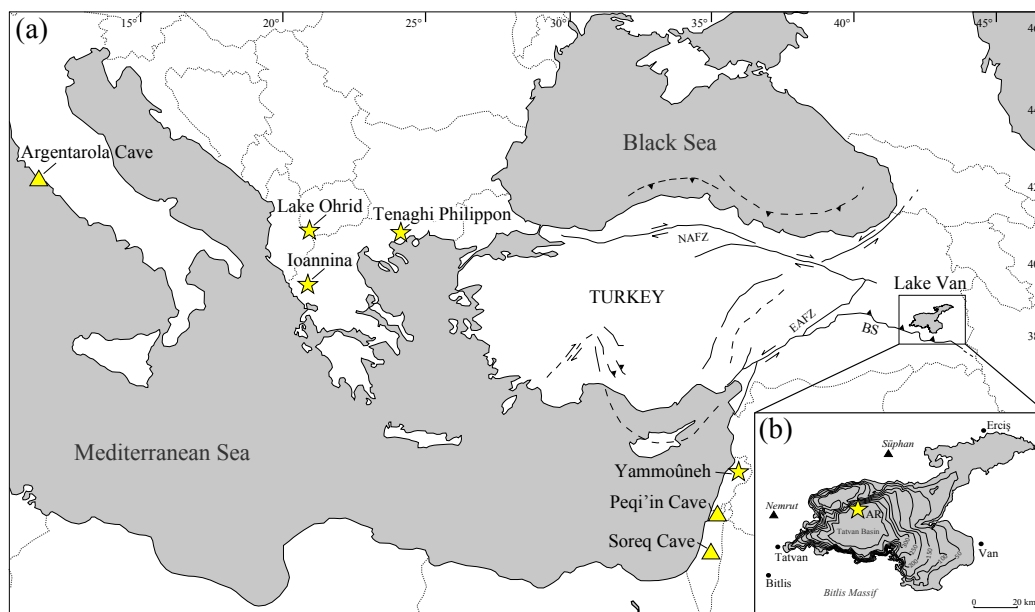
- 518 Schwander, J., Selmo, E., Souchez, R., Spahni, R., Stauffer, B., Steffensen, J.P., Stenni, B.,
 519 Stocker, T.F., Tison, J.L., Werner, M., Wolff, E.W., 2007. Orbital and Millennial Antarctic
 520 Climate Variability over the Past 800,000 Years. *Science* 317, 793–796.
 521 doi:10.1126/science.1141038
- 522 Kallel, N., Duplessy, J.-C., Labeyrie, L., Fontugne, M., Paterne, M., Montacer, M., 2000. Mediterranean
 523 pluvial periods and sapropel formation over the last 200 000 years. *Palaeogeography,*
 524 *Palaeoclimatology, Palaeoecology* 157, 45–58. doi:10.1016/S0031-0182(99)00149-2
- 525 Kwiecien, O., Stockhecke, M., Pickarski, N., Heumann, G., Litt, T., Sturm, M., Anselmetti, F., Kipfer, R.,
 526 Haug, G.H., 2014. Dynamics of the last four glacial terminations recorded in Lake Van, Turkey.
 527 *Quaternary Science Reviews* 104, 42–52. doi:10.1016/j.quascirev.2014.07.001
- 528 Lang, N., Wolff, E.W., 2011. Interglacial and glacial variability from the last 800 ka in marine, ice and
 529 terrestrial archives. *Climate of the Past* 7, 361–380. doi:10.5194/cp-7-361-2011
- 530 Lemcke, G., Sturm, M., 1997. δ 18O and trace element measurements as proxy for the reconstruction of
 531 climate changes at Lake Van (Turkey): preliminary results., in: Dalfes, H.N., Kulka, G., Weiss, H.
 532 (Eds.), *Third Millennium BC Climate Change and Old World Collapse*. NATO ASI Series, pp.
 533 653–679.
- 534 Leng, M.J., Marshall, J.D., 2004. Palaeoclimate interpretation of stable isotope data from lake sediment
 535 archives. *Quaternary Science Reviews* 23, 811–831. doi:10.1016/j.quascirev.2003.06.012
- 536 Litt, T., Anselmetti, F.S., 2014. Lake Van deep drilling project PALEOVAN. *Quaternary Science*
 537 *Reviews* 104, 1–7. doi:10.1016/j.quascirev.2014.09.026
- 538 Litt, T., Anselmetti, F.S., Baumgarten, H., Beer, J., Çagatay, N., Cukur, D., Damci, E., Glombitza, C.,
 539 Haug, G., Heumann, G., Kallmeyer, J., Kipfer, R., Krastel, S., Kwiecien, O., Meydan, A.F.,
 540 Orcen, S., Pickarski, N., Randlett, M.-E., Schmincke, H.-U., Schubert, C.J., Sturm, M., Sumita,
 541 M., Stockhecke, M., Tomonaga, Y., Vigliotti, L., Wonik, T., team, the P. scientific, 2012.
 542 500,000 Years of Environmental History in Eastern Anatolia: The PALEOVAN Drilling Project.
 543 *Scientific Drilling Journal* 18–29. doi:10.5194/sd-14-18-2012
- 544 Litt, T., Krastel, S., Sturm, M., Kipfer, R., Örcen, S., Heumann, G., Franz, S.O., Ülgen, U.B., Niessen, F.,
 545 2009. “PALEOVAN”, International Continental Scientific Drilling Program (ICDP): site survey
 546 results and perspectives. *Quaternary Science Reviews* 28, 1555–1567.
 547 doi:10.1016/j.quascirev.2009.03.002
- 548 Litt, T., Pickarski, N., Heumann, G., Stockhecke, M., Tzedakis, P.C., 2014. A 600,000 year long
 549 continental pollen record from Lake Van, eastern Anatolia (Turkey). *Quaternary Science Reviews*
 550 104, 30–41. doi:10.1016/j.quascirev.2014.03.017
- 551 Margari, V., Skinner, L.C., Tzedakis, P.C., Ganopolski, A., Vautravers, M., Shackleton, N.J., 2010. The
 552 nature of millennial-scale climate variability during the past two glacial periods. *Nature*
 553 *Geoscience* 3, 127–131. doi:10.1038/geo740
- 554 Martinson, D.G., Pisias, N.G., Hays, J.D., Imbrie, J., Moore Jr., T.C., Shackleton, N.J., 1987. Age dating
 555 and the orbital theory of the ice ages: Development of a high-resolution 0 to 300,000-year
 556 chronostratigraphy. *Quaternary Research* 27, 1–29. doi:10.1016/0033-5894(87)90046-9
- 557 McManus, J.F., Oppo, D.W., Cullen, J.L., 1999. A 0.5-Million-Year Record of Millennial-Scale Climate
 558 Variability in the North Atlantic. *Science* 283, 971–975. doi:10.1126/science.283.5404.971
- 559 Milner, A.M., Müller, U.C., Roucoux, K.H., Collier, R.E.L., Pross, J., Kalaitzidis, S., Christianis, K.,
 560 Tzedakis, P.C., 2013. Environmental variability during the Last Interglacial: a new high-
 561 resolution pollen record from Tenaghi Philippon, Greece. *Journal of Quaternary Science* 28, 113–
 562 117. doi:10.1002/jqs.2617
- 563 Moore, P.D., Webb, J.A., Collinson, M.E., 1991. *Pollen Analysis*. Blackwell Science.
- 564 NGRIP, 2004. High-resolution record of Northern Hemisphere climate extending into the last interglacial
 565 period. *Nature* 431, 147–151. doi:10.1038/nature02805
- 566 Petit, J.R., Jouzel, J., Raynaud, D., Barkov, N.I., Barnola, J.-M., Basile, I., Bender, M., Chappellaz, J.,
 567 Davis, M., Delaygue, G., Delmotte, M., Kotlyakov, V.M., Legrand, M., Lipenkov, V.Y., Lorius,
 568 C., Pepin, L., Ritz, C., Saltzman, E., Stievenard, M., 1999. Climate and atmospheric history of the
 569 past 420,000 years from the Vostok ice core, Antarctica. *Nature* 399, 429–436. doi:10.1038/20859



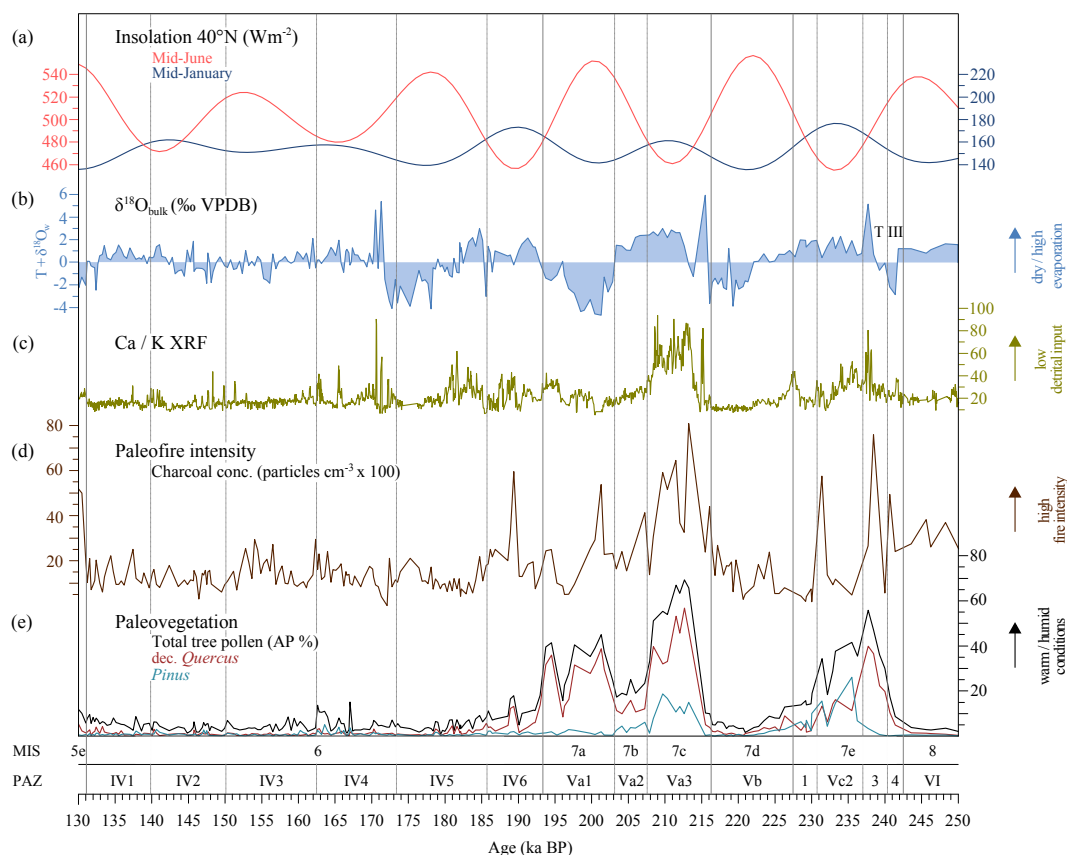
- 570 Pickarski, N., Kwiecien, O., Djamali, M., Litt, T., 2015a. Vegetation and environmental changes during
571 the last interglacial in eastern Anatolia (Turkey): a new high-resolution pollen record from Lake
572 Van. *Palaeogeography, Palaeoclimatology, Palaeoecology* 145–158.
573 doi:10.1016/j.palaeo.2015.06.015
- 574 Pickarski, N., Kwiecien, O., Langgut, D., Litt, T., 2015b. Abrupt climate and vegetation variability of
575 eastern Anatolia during the last glacial. *Climate of the Past* 11, 1491–1505. doi:10.5194/cp-11-
576 1491-2015
- 577 Punt, W., 1976. *The Northwest European Pollen Flora*. Elsevier, Amsterdam.
- 578 Rasmussen, S.O., Bigler, M., Blockley, S.P., Blunier, T., Buchardt, S.L., Clausen, H.B., Cvijanovic, I.,
579 Dahl-Jensen, D., Johnsen, S.J., Fischer, H., Gkinis, V., Guillevic, M., Hoek, W.Z., Lowe, J.J.,
580 Pedro, J.B., Popp, T., Seierstad, I.K., Steffensen, J.P., Svensson, A.M., Vallelonga, P., Vinther,
581 B.M., Walker, M.J.C., Wheatley, J.J., Winstrup, M., 2014. A stratigraphic framework for abrupt
582 climatic changes during the Last Glacial period based on three synchronized Greenland ice-core
583 records: refining and extending the INTIMATE event stratigraphy. *Quaternary Science Reviews*
584 106, 14–28. doi:10.1016/j.quascirev.2014.09.007
- 585 Reilinger, R., McClusky, S., Vernant, P., Lawrence, S., Ergintav, S., Cakmak, R., Ozener, H., Kadirov, F.,
586 Guliev, I., Stepanyan, R., Nadariya, M., Hahubia, G., Mahmoud, S., Sakr, K., ArRajehi, A.,
587 Paradissis, D., Al-Aydrus, A., Prilepin, M., Guseva, T., Evren, E., Dmitrova, A., Filikov, S.V.,
588 Gomez, F., Al-Ghazzi, R., Karam, G., 2006. GPS constraints on continental deformation in the
589 Africa-Arabia-Eurasia continental collision zone and implications for the dynamics of plate
590 interactions. *Journal of Geophysical Research* 111, 1–26. doi:10.1029/2005JB004051
- 591 Reille, M., 1999. Pollen et spores d'Europe et d'Afrique du Nord. *Laboratoire de Botanique Historique et*
592 *Palynologie, Marseille*.
- 593 Reille, M., 1998. Pollen et spores d'Europe et d'Afrique du Nord (Supplement 2). *Laboratoire de*
594 *Botanique Historique et Palynologie, Marseille*.
- 595 Reille, M., 1995. Pollen et spores d'Europe et d'Afrique du Nord (Supplement 1). *Laboratoire de*
596 *Botanique Historique et Palynologie, Marseille*.
- 597 Roberts, N., Jones, M.D., Benkaddour, A., Eastwood, W.J., Filippi, M.L., Frogley, M.R., Lamb, H.F.,
598 Leng, M.J., Reed, J.M., Stein, M., Stevens, L., Valero-Garcés, B., Zanchetta, G., 2008. Stable
599 isotope records of Late Quaternary climate and hydrology from Mediterranean lakes: the
600 ISOMED synthesis. *Quaternary Science Reviews* 27, 2426–2441.
601 doi:10.1016/j.quascirev.2008.09.005
- 602 Roucoux, K.H., Tzedakis, P.C., Frogley, M.R., Lawson, I.T., Preece, R.C., 2008. Vegetation history of the
603 marine isotope stage 7 interglacial complex at Ioannina, NW Greece. *Quaternary Science Reviews*
604 27, 1378–1395. doi:10.1016/j.quascirev.2008.04.002
- 605 Roucoux, K.H., Tzedakis, P.C., Lawson, I.T., Margari, V., 2011. Vegetation history of the penultimate
606 glacial period (Marine isotope stage 6) at Ioannina, north-west Greece. *Journal of Quaternary*
607 *Science* 26, 616–626. doi:10.1002/jqs.1483
- 608 Sadori, L., Koutsodendris, A., Panagiotopoulos, K., Masi, A., Bertini, A., Combourieu-Nebout, N.,
609 Francke, A., Kouli, K., Joannin, S., Mercuri, A.M., Peyron, O., Torri, P., Wagner, B., Zanchetta,
610 G., Sinopoli, G., Donders, T.H., 2016. Pollen-based paleoenvironmental and paleoclimatic change
611 at Lake Ohrid (south-eastern Europe) during the past 500 ka. *Biogeosciences* 13, 1423–1437.
612 doi:10.5194/bg-13-1423-2016
- 613 Shackleton, N.J., Hall, M.A., Vincent, E., 2000. Phase relationships between millennial-scale events
614 64,000–24,000 years ago. *Paleoceanography* 15, 565–569. doi:10.1029/2000PA000513
- 615 Shumilovskikh, L.S., Tarasov, P., Arz, H.W., Fleitmann, D., Marret, F., Nowaczyk, N., Plessen, B.,
616 Schlüt, F., Behling, H., 2012. Vegetation and environmental dynamics in the southern Black Sea
617 region since 18 kyr BP derived from the marine core 22-GC3. *Palaeogeography,*
618 *Palaeoclimatology, Palaeoecology* 337–338, 177–193. doi:10.1016/j.palaeo.2012.04.015
- 619 Stockhecke, M., Kwiecien, O., Vigliotti, L., Anselmetti, F.S., Beer, J., Çağatay, M.N., Channell, J.E.T.,
620 Kipfer, R., Lachner, J., Litt, T., Pickarski, N., Sturm, M., 2014a. Chronostratigraphy of the



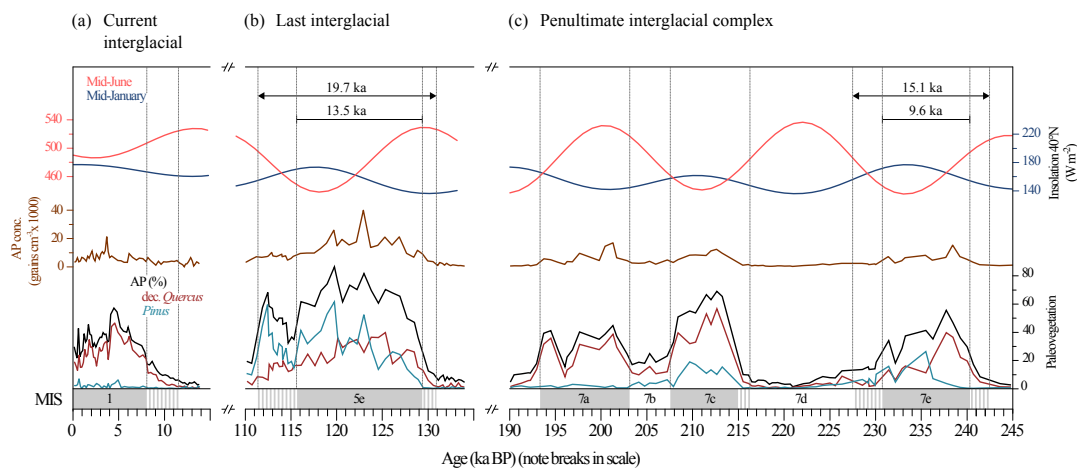
- 621 600,000 year old continental record of Lake Van (Turkey). *Quaternary Science Reviews* 104, 8–
 622 17. doi:10.1016/j.quascirev.2014.04.008
- 623 Stockhecke, M., Sturm, M., Brunner, I., Schmincke, H.-U., Sumita, M., Kipfer, R., Cukur, D., Kwiecien,
 624 O., Anselmetti, F.S., 2014b. Sedimentary evolution and environmental history of Lake Van
 625 (Turkey) over the past 600 000 years. *Sedimentology* 61, 1830–1861. doi:10.1111/sed.12118
- 626 Stockmarr, J., 1971. Tablets with spores used in absolute pollen analysis. *Pollen et Spores* 13, 615–621.
- 627 Thouveny, N., Carcaillet, J., Moreno, E., Leduc, G., Nérini, D., 2004. Geomagnetic moment variation and
 628 paleomagnetic excursions since 400 kyr BP: a stacked record from sedimentary sequences of the
 629 Portuguese margin. *Earth and Planetary Science Letters* 219, 377–396. doi:10.1016/S0012-
 630 821X(03)00701-5
- 631 Tzedakis, P.C., 2005. Towards an understanding of the response of southern European vegetation to
 632 orbital and suborbital climate variability. *Quaternary Science Reviews* 24, 1585–1599.
 633 doi:10.1016/j.quascirev.2004.11.012
- 634 Tzedakis, P.C., 1994. Hierarchical biostratigraphical classification of long pollen sequences. *Journal of*
 635 *Quaternary Science* 9, 257–259. doi:10.1002/jqs.3390090306
- 636 Tzedakis, P.C., Frogley, M.R., Heaton, T.H.E., 2003a. Last Interglacial conditions in southern Europe:
 637 evidence from Ioannina, northwest Greece. *Global and Planetary Change* 36, 157–170.
 638 doi:10.1016/S0921-8181(02)00182-0
- 639 Tzedakis, P.C., Hooghiemstra, H., Palike, H., 2006. The last 1.35 million years at Tenaghi Philippon:
 640 revised chronostratigraphy and long-term vegetation trends. *Critical Quaternary Stratigraphy* 25,
 641 3416–3430. doi:10.1016/j.quascirev.2006.09.002
- 642 Tzedakis, P.C., Lawson, I.T., Frogley, M.R., Hewitt, G.M., Preece, R.C., 2002. Buffered Tree Population
 643 Changes in a Quaternary Refugium: Evolutionary Implications. *Science* 297, 2044–2047.
 644 doi:10.1126/science.1073083
- 645 Tzedakis, P.C., McManus, J.F., Hooghiemstra, H., Oppo, D.W., Wijmstra, T.A., 2003b. Comparison of
 646 changes in vegetation in northeast Greece with records of climate variability on orbital and
 647 suborbital frequencies over the last 450 000 years. *Earth and Planetary Science Letters* 212, 197–
 648 212. doi:10.1016/S0012-821X(03)00233-4
- 649 Vigliotti, L., Channell, J.E.T., Stockhecke, M., 2014. Paleomagnetism of Lake Van sediments: chronology
 650 and paleoenvironment since 350 ka. *Quaternary Science Reviews* 104, 18–29.
 651 doi:10.1016/j.quascirev.2014.09.028
- 652 Wick, L., Lemcke, G., Sturm, M., 2003. Evidence of Lateglacial and Holocene climatic change and
 653 human impact in eastern Anatolia: high resolution pollen, charcoal, isotopic and geochemical
 654 records from the laminated sediments of Lake Van. *The Holocene* 13, 665–675.
 655 doi:10.1191/0959683603hl653rp
- 656 Wolff, E.W., Chappellaz, J., Blunier, T., Rasmussen, S.O., Svensson, A., 2010. Millennial-scale
 657 variability during the last glacial: The ice core record. *Quaternary Science Reviews* 29, 2828–
 658 2838. doi:10.1016/j.quascirev.2009.10.013
- 659 Zohary, M., 1973. *Geobotanical Foundations of the Middle East*. Gustav Fischer Verlag, Swets &
 660 Zeitlinger. Stuttgart, Amsterdam.
 661



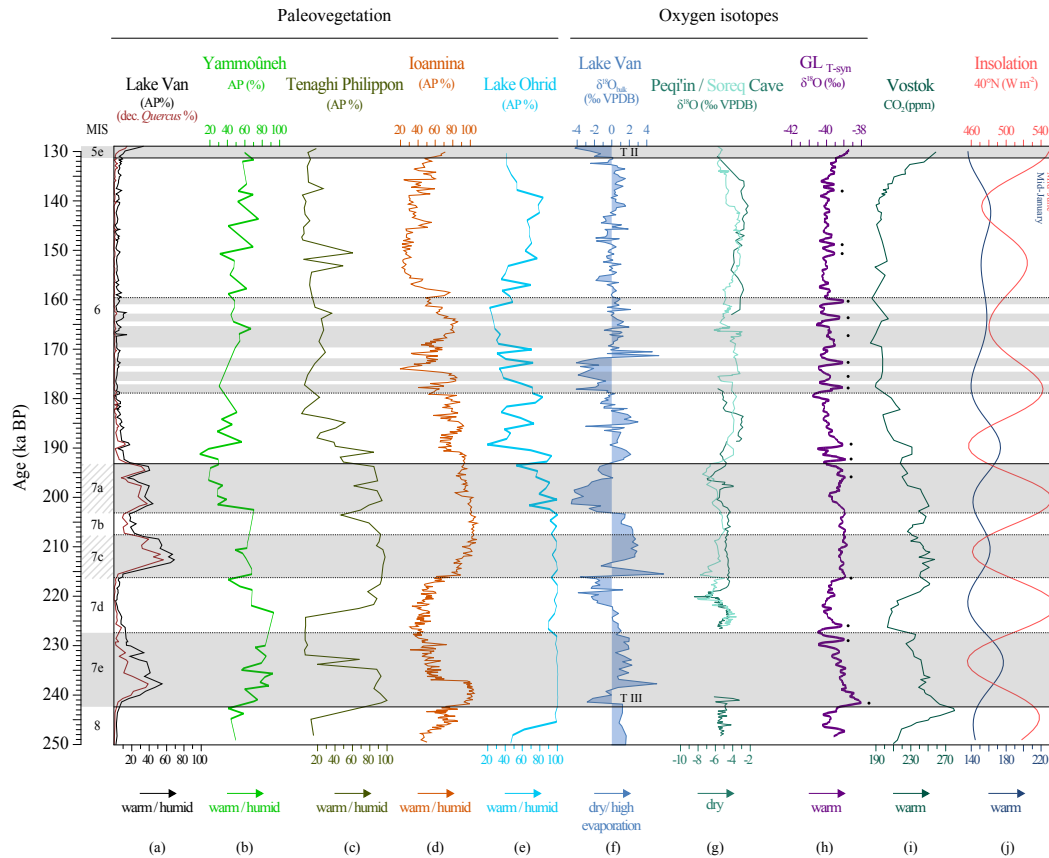
662 **Fig. 1:** Map of the eastern Mediterranean region showing major tectonic structures in Turkey (a) Location of key
663 Mediterranean and Near East pollen sites (stars) and speleothem records (triangle) mentioned in the text. (b)
664 Bathymetry of Lake Van including the Ahlat Ridge drill site (AR). The black triangle indicates the positions of the
665 active Nemrut and Süphan volcanoes. NAFZ: North Anatolian Fault Zone; EAFZ: East Anatolian Fault Zone; BS:
666 Bitlis Suture.



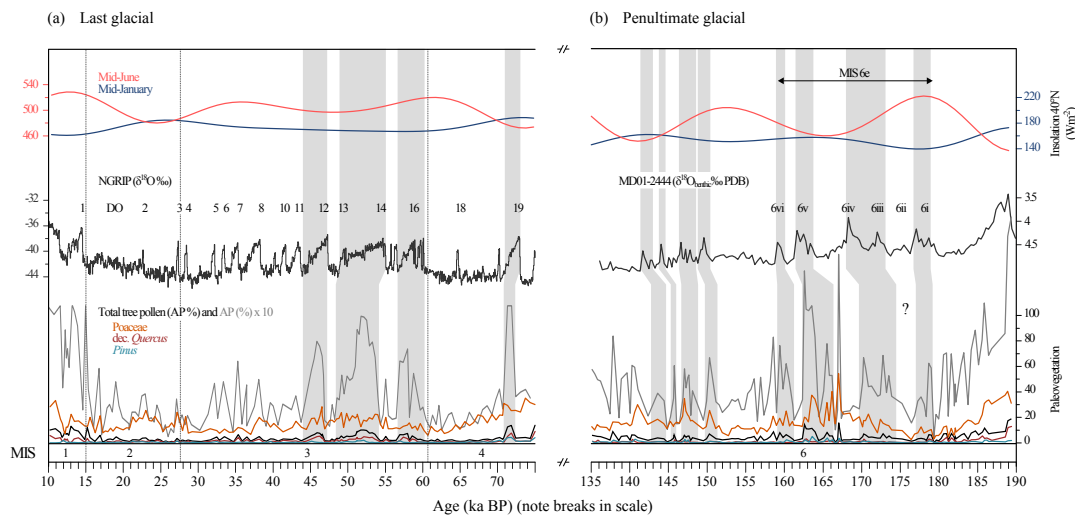
677 **Fig. 3:** Comparative study of Lake Van paleoenvironmental proxies during the penultimate interglacial glacial
 678 cycle. (a) Insolation values (40°N , Wm^{-2}) after Berger (1978) and Berger et al. (2007); (b) Lake Van oxygen isotope
 679 records $\delta^{18}\text{O}_{\text{bulk}}$ (‰ VPDB; new analyzed isotope data including the already published isotope record by Kwiecien
 680 et al., 2014); (c) Calcium/potassium ratio (Ca/K) after Kwiecien et al. (2014); (d) Fire intensity at Lake Van (>20
 681 μm , charcoal concentration in particles cm^{-3}); (e) Selected tree percentages (total arboreal pollen (AP), deciduous
 682 *Quercus*, and *Pinus*) including the pollen data from Litt et al. (2014). MIS – Marine Isotope Stage; PAZ – Pollen
 683 assemblage zone. Termination III (T III) at 241.4 ka BP is indicated.
 684



685 **Fig. 4:** Comparison of (a) Current interglacial (MIS 1; Litt et al., 2009) with (b) Last interglacial (MIS 5e; Pickarski
 686 et al., 2015a), and (c) Penultimate interglacial complex (MIS 7; this study) at Lake Van. Shown is the insolation
 687 values (40°N , Wm^{-2}) after Berger (1978) and Berger et al. (2007), the Lake Van arboreal pollen (AP) concentration
 688 (grains cm^{-3} , brown line), and the Lake Van paleovegetation (AP, deciduous *Quercus*, and *Pinus* in %). The grey
 689 boxes mark each steppe-forest intervals. Marine Isotope Stage (MIS) and the length of each full interglacial (MIS
 690 5e, 7e, black arrows) are indicated.
 691



692 **Fig. 5:** Correlation scheme of Lake Van pollen record with terrestrial, marine and ice core paleoclimatic sequences.
 693 (a) Total arboreal pollen (AP %) and deciduous *Quercus* curve from Lake Van (this study); (b) Arboreal pollen
 694 percentages from Yammoûneh basin (Lebanon; Gasse et al., 2015); (c) Tree percentages of the Tenaghi Philippon
 695 record (NE Greece; Tzedakis et al., 2003b); (d) AP sequence from Ioannina basin (NW Greece; Roucoux et al.,
 696 2011, 2008); (e) Lake Ohrid pollen record (AP %; Macedonia, Albania; Sadori et al., 2016); (f) Stable oxygen
 697 isotope record of Lake Van ($\delta^{18}\text{O}_{\text{bulk}}$ data including the already published isotope record of Kwiecien et al., 2014);
 698 (g) Peqi'in and Soreq Cave speleothem records (Israel; M. Bar-Matthews & A. Ayalon, unpubl. data); (h) Synthetic
 699 Greenland ice-core record (GLT-syn; Barker et al., 2011); (i) Atmospheric CO_2 concentration from Vostok ice core,
 700 Antarctica (Petit et al., 1999); (j) Mid-June and Mid-January insolation for 40°N (Berger, 1978; Berger et al., 2007).
 701 Marine Isotope Stages is also shown (MIS; Martinson et al., 1987). Bands highlights periods of distinctive climate
 702 signature discussed in the text. Black dots mark significant interstadial periods. Terminations (T III and T II) are
 703 indicated.
 704



705 **Fig. 6:** Comparison of the (a) Last glacial period (MIS 4-2; Pickarski et al., 2015b) with the (b) Penultimate glacial
 706 (this study) characteristics at Lake Van. Shown is the insolation values (40°N, Wm^{-2}) after Berger (1978) and Berger
 707 et al. (2007), the $\delta^{18}O$ profile from NGRIP ice core (Greenland; NGRIP members, 2004) labeled with Dansgaard-
 708 Oeschger (DO) events 1 to 19 for the last glacial period, the $\delta^{18}O$ composition of benthic foraminifera of the marine
 709 core MD01-2444 (Portuguese margin; Margari et al., 2010) for the penultimate glacial, and the Lake Van
 710 paleovegetation with AP % (shown in black), AP in 10-fold exaggeration (grey line), Poaceae, deciduous *Quercus*,
 711 and *Pinus*. The grey boxes mark the correlation between the different paleoenvironmental records of pronounced
 712 interstadial oscillations. Marine Isotope Stage (MIS) and informally numbered interstadials of the MD01-2444
 713 record are indicated.

714
 715
 716
 717
 718



719 **Tables:**

720 **Table 1:** Present-day climate data at Lake Van (see Fig. 1 for the location; Climate-data.org; 1982-2012).

Station	Coordinates			Mean temperature (°C)			Mean precipitation (mm)		
	Latitude (°N)	Longitude (°E)	Altitude (m asl)	Jan.	July	Year	Jan.	July	Year
Bitlis	38°24'	42°60'	1536	-2.8	22.5	9.7	131	5	1059
Tatvan	38°30'	42°17'	1651	-2.5	21.3	9.0	89	6	844
Erciş	39°20'	43°22'	1691	-4.9	21.8	8.5	38	8	499
Van	38°27'	43°19'	1689	-3.7	21.2	8.9	37	5	409

721

722 **Table 2:** Main palynological characteristics of the Lake Van pollen assemblage superzones (PAS) and
 723 zones (PAZ) with composite depth (mcbf), age (ka BP), criteria for lower boundary, components of the
 724 pollen assemblage (AP: arboreal pollen, NAP: non-arboreal pollen), green algae concentration (GA: low
 725 <1,000; high >1,000 coenobia cm⁻³), dinoflagellates concentrations (DC: low: <100; high: >100 cysts cm⁻³
 726 ³), charcoal concentrations (CC: low: <2,000; moderate: 2,000-4,000; high: >4,000 particles cm⁻³) and
 727 their inferred dominated vegetation type during the penultimate interglacial-glacial cycle. Marine Isotope
 728 Stages (MIS) after Martinson et al. (1987) were shown on the right.



PAS	PAZ	Composite depth (mcbf)	Age (ka BP)	Criteria for lower boundary	Main palynological characteristics (minimum – maximum in %)	Dominant vegetation type	MIS
IIIc	6	57.20 - 58.09	129.1 – 131.21	Occurrence <i>Pistacia</i>	AP: <i>Betula</i> (2-4 %), dec. <i>Quercus</i> (1-13 %), <i>Ephedra distachya</i> -type (0-3 %), <i>Ulmus</i> (0-2 %), <i>Juniperus</i> (0-1 %), <i>Pinus</i> (0-1 %), <i>Pistacia cf. atlantica</i> (0-1 %) NAP: <i>Artemisia</i> (16-49 %), Poaceae (7-25 %), Chenopodiaceae (2-52 %) GA: Low DC: Low CC: Moderate to high	Steppe taxa become less widespread, giving way to open grassland	5e
IV	1	58.09 - 63.25	131.21 - 139.87	Chenopodiaceae >40 %	AP: Low AP (2-8 %); increased frequencies of <i>Ephedra distachya</i> -type (1-5 %); deciduous <i>Quercus</i> , <i>Betula</i> , <i>Pinus</i> , and <i>Juniperus</i> are abundant at low level NAP: Chenopodiaceae (39-64 %) show high values at the top of sub-zone, while <i>Artemisia</i> (8-29 %) abundances rapidly decline; still moderate Poaceae percentages GA: Low DC: Low CC: Low to moderate	Open desert steppe vegetation	6
	2	63.25 - 71.50	139.87 - 150.14	Chenopodiaceae <40 %	AP: Low AP (1-7 %); temperate trees are present at low level NAP: Expansion of <i>Artemisia</i> continues and peaks in the middle of the sub-zone (54 %); Chenopodiaceae percentages drop to 15-41 %; moderate Poaceae values (11-34 %), GA: Low with a single peak at 146.4 ka BP (c. 3,700 coenobia cm ³) DC: Low CC: Low	Productive dwarf shrub steppe vegetation	
	3	71.50 - 77.72	150.14 - 162.49	Chenopodiaceae >40 %; decrease <i>Quercus</i>	AP: Deciduous <i>Quercus</i> , <i>Betula</i> , <i>Pinus</i> , and <i>Juniperus</i> are continuously present at low level (AP 2-8 %); increase of <i>Ephedra distachya</i> -type (1-6 %) NAP: Predominance of Chenopodiaceae (33-62 %); <i>Artemisia</i> (6-38 %) shows moderate values with increasing trend towards the top, Poaceae continuously present at ~13 % GA: High to low at the end of the sub-zone DC: Low to high CC: Low to moderate	Open desert steppe vegetation	
	4	77.72 - 83.84	162.49 - 173.38	Chenopodiaceae <40 %; increase <i>Quercus</i>	AP: Low AP (1-14 %); relatively moderate contents of deciduous <i>Quercus</i> (0-3 %); slight decrease of <i>Betula</i> (0-2 %), while <i>Pinus</i> (0-5 %) and <i>Juniperus</i> (0-1 %) percentages increase towards at the end of the sub-zone NAP: Predominance of <i>Artemisia</i> (10-46 %) and Poaceae (8-54 %); Chenopodiaceae abundances (5-40 %) are reduced within this sub-zone GA: Low to high DC: Low CC: Low with moderate peaks at the end	Fluctuation between open desert-steppe and grassland scattered with temperate trees	
	5	83.84 - 93.51	173.38 - 185.74	Chenopodiaceae >40 %	AP: AP (1-9 %) decrease continuously throughout the sub-zone; mainly by deciduous <i>Quercus</i> (0-4 %)	Change from grassland to desert steppe	



PAS	PAZ	Composite depth (mcbf)	Age (ka BP)	Criteria for lower boundary	Main palynological characteristics (minimum – maximum in %)	Dominant vegetation type	MIS
					<p>NAP: Base marked by a pronounced expansion of <i>Chenopodiaceae</i> (33-64 %); <i>Artemisia</i> continues from previous sub-zone with max. 32 %, while <i>Poaceae</i> decrease (3-18 %)</p> <p>GA: Low DC: Low to high towards the top CC: Low</p>	vegetation at the end of the zone	
	6	93.51 - 97.02	185.74 - 193.36	Decrease <i>Quercus</i> ; increase <i>Poaceae</i>	<p>AP: General reduction of AP percentages throughout the sub-zone; still abundant: deciduous <i>Quercus</i> (1-31 %), <i>Betula</i> (0-2 %), and <i>Ulmus</i> (<1 %); conifer trees maintain moderate values with small oscillations; disappearance of <i>Pistacia cf. atlantica</i></p> <p>NAP: Pronounced increase of <i>Poaceae</i> (21-45 %) values; steppic herbs continue to be moderate</p> <p>GA: Low DC: Low CC: Low to moderate, peak at 189.4 ka BP</p>	Open grasslands with scattered temperate trees	
Va	1	97.02 - 99.88	193.36 - 203.11	Increase AP; peak <i>Pistacia</i>	<p>AP: High AP (24-44 %) percentages mainly of deciduous <i>Quercus</i> (8-38 %), increasing values of <i>Betula</i> (0-4 %), <i>Pinus</i> (0-3 %), and <i>Juniperus</i> (0-3 %); peak of <i>Pistacia cf. atlantica</i> (c. 3 %) at the beginning of the sub-zone; high tree concentration (>3,000 grains cm⁻³)</p> <p>NAP: Moderate percentages of steppic herbs (<i>Artemisia</i> 13-29 % and <i>Chenopodiaceae</i> 11-33 %) with significant peak of NAP (85 %) near the base</p> <p>GA: Low DC: Low CC: Low to moderate with one single high peak at 201.3 ka BP (>5,000 particles cm⁻³)</p>	Expansion of oak steppe-forest along with Mediterranean taxa (<i>Pistacia</i>), short-term influence of steppe vegetation	7a
	2	99.88 - 101.30	203.11 - 207.56	AP <40 %; decrease <i>Quercus</i>	<p>AP: Reduction of tree & shrubs (AP 17-50 %) mainly by deciduous <i>Quercus</i> (10-30 %) and <i>Pinus</i> (1-8 %) but still above 15 %; increase of <i>Ephedra distachya</i>-type (1-3 %) and <i>Betula</i> (0-2 %)</p> <p>NAP: Rapid expansion of <i>Chenopodiaceae</i> (15-47 %), peak values for <i>Artemisia</i> (9-32 %) at the beginning; moderate <i>Poaceae</i> (5-19 %) values</p> <p>GA: Low DC: Low to high CC: Low to moderate</p>	More open (steppe) landscape with still patchy pioneer & temperate tree	7b
	3	101.30 - 104.19	207.56 - 216.28	<i>Chenopodiaceae</i> <40 %; increase <i>Quercus</i>	<p>AP: Predominance of deciduous <i>Quercus</i> (2-56 %) with significant peak at 102.8 mcbf (212.6 ka BP) followed by a decreasing trend; high values of <i>Pinus</i> (0-19 %); <i>Betula</i> (0-4 %) and <i>Juniperus</i> (0-2 %) are abundant; <i>Pistacia cf. atlantica</i> and <i>Ulmus</i> pollen occur sporadically; high tree concentration (>3,000 grains cm⁻³)</p> <p>NAP: Peak of <i>Artemisia</i> (6-38 %), <i>Poaceae</i> (5-21 %), and <i>Tubuliflorae</i> (2-13 %) percentages at the beginning of the sub-zone; very low <i>Chenopodiaceae</i> values (4-48 %)</p>	Expansion of oak-pine steppe-forest	7c



PAS	PAZ	Composite depth (mcbflf)	Age (ka BP)	Criteria for lower boundary	Main palynological characteristics (minimum – maximum in %)	Dominant vegetation type	MIS
GA: Low DC: No occurrence CC: High							
Vb		104.19 - 109.05	216.28 - 227.42	Chenopodiaceae >40 %	AP: Very low tree percentages (1-12 %) and tree concentration (<2,000 grains cm ⁻³); decrease of deciduous <i>Quercus</i> (0-9 %), <i>Pinus</i> (0-3 %), and <i>Juniperus</i> (<1 %) NAP: Predominance of Chenopodiaceae (37-76 %); Poaceae (4-15 %), and <i>Artemisia</i> (6-26 %) are abundant GA: Low DC: Low CC: Low with moderate values at the end of this zone	Extensive desert steppe vegetation	7d
Vc	1	109.05 - 109.94	227.42 - 230.71	Disappearance <i>Pistacia</i> ; decrease AP, increase Chenopodiaceae	AP: Continuous decrease in AP (14-19 %), mainly deciduous <i>Quercus</i> (2-5 %), <i>Pinus</i> (2-10 %); <i>Pistacia</i> cf. <i>atlantica</i> disappears NAP: Strong increase in Chenopodiaceae (23-32 %) abundances, moderate reduction of <i>Artemisia</i> (19-27 %) and Poaceae (18-26 %) GA: Low DC: Low CC: Low	Increasing influence of steppe taxa, expansion of open vegetation	7e
	2	109.94 - 111.73	230.71 - 236.95	Decrease <i>Quercus</i> and <i>Pistacia</i> ; increase <i>Pinus</i>	AP: Percentages of deciduous <i>Quercus</i> (6-21 %), <i>Betula</i> (0-1 %) and <i>Pistacia</i> cf. <i>atlantica</i> decline while those of <i>Pinus</i> (4-26 %) and <i>Juniperus</i> (2-5 %) rise NAP: Steppe taxa expand, mainly <i>Artemisia</i> (5-26 %) and Poaceae (21-36 %), still low Chenopodiaceae (3-13 %) percentages GA: High DC: Low CC: Low with one peak at the end of the sub-zone.	All temperate tree taxa declined gradually, while <i>Pinus</i> and grassland expanded (Pinus-dominated steppe-forest)	
	3	111.73 - 112.64	236.95 - 240.31	<i>Quercus</i> >10 %; Chenopodiaceae <40 %	AP: Peak values for <i>Betula</i> (4-8 %) and <i>Pistacia</i> cf. <i>atlantica</i> (1-2 %), rapid expansion of deciduous <i>Quercus</i> (10-40 %); <i>Pinus</i> (0-3 %), <i>Juniperus</i> (0-1 %), and <i>Ulmus</i> are abundant; highest tree concentration (c. 5,300-15,300 grains cm ⁻³) during that PAZ NAP: Retreat in steppe percentages mainly <i>Artemisia</i> (13-37 %) Chenopodiaceae (3-6 %); moderate Poaceae values (12-20 %) GA: Low DC: No occurrence CC: Moderate to high	Expansion of oak steppe-forest along with Mediterranean sclerophylls (<i>Pistacia</i>)	
	4	112.64 - 113.70	240.31 - 242.48	Occurrence <i>Pistacia</i>	AP: Increase in temperate trees & shrubs, in particular deciduous <i>Quercus</i> (1-10 %) and <i>Betula</i> (1-5 %); occurrence of <i>Pistacia</i> cf. <i>atlantica</i> (~1 %), <i>Juniperus</i> (~1 %), and <i>Ulmus</i> (sporadic) NAP: Herbaceous taxa continue, mainly Poaceae (7-20 %) and <i>Artemisia</i> (37-56 %); pronounced decrease in Chenopodiaceae (6-59 %) GA: Low DC: No occurrence CC:	Steppe taxa become less widespread, giving way to open grassland	



PAS	PAZ	Composite depth (mcbf)	Age (ka BP)	Criteria for lower boundary	Main palynological characteristics (minimum – maximum in %)	Dominant vegetation type	MIS
Moderate to high							
VI		113.70 - 118.18	242.48 - 250.14	Not defined	<p>AP: Very low abundances of arboreal pollen percentages (<i>Betula</i> 0-1 % and deciduous <i>Quercus</i> 0-1 %), very low tree concentration (c. 570-1,320 grains cm⁻³)</p> <p>NAP: Predominance of steppe taxa, mainly <i>Chenopodiaceae</i> (52-66 %) and <i>Artemisia</i> (18-33 %)</p> <p>GA: Low DC: Low CC: Moderate</p>	Extensive open desert-steppe vegetation	8